

1-1-1996

Vectorial Quadratic Interactions For All-Optical Signal Processing Via Second-Harmonic Generation

G. Assanto

D. J. Hagan
University of Central Florida

G. I. Stegeman
University of Central Florida

Eric W. Van Stryland
University of Central Florida

W. E. Torruellas

Find similar works at: <https://stars.library.ucf.edu/facultybib1990>
University of Central Florida Libraries <http://library.ucf.edu>

This Article; Proceedings Paper is brought to you for free and open access by the Faculty Bibliography at STARS. It has been accepted for inclusion in Faculty Bibliography 1990s by an authorized administrator of STARS. For more information, please contact STARS@ucf.edu.

Recommended Citation

Assanto, G.; Hagan, D. J.; Stegeman, G. I.; Van Stryland, Eric W.; and Torruellas, W. E., "Vectorial Quadratic Interactions For All-Optical Signal Processing Via Second-Harmonic Generation" (1996). *Faculty Bibliography 1990s*. 3086.
<https://stars.library.ucf.edu/facultybib1990/3086>

Vectorial quadratic interactions for all-optical signal processing via second-harmonic generation

G. ASSANTO

Department of Electronic Engineering, Terza University of Rome, Via della Vasca Navale 84, 00146 Rome, Italy.

D. J. HAGAN, G. I. STEGEMAN, E. W. VAN STRYLAND

Center for Research and Education in Optics and Lasers, University of Central Florida, Orlando, FL 32816-2700, USA.

W. E. TORRUELLAS

Department of Physics, Washington State University, Pullman, WA 99164-2814, USA.

Quadratic interactions involving three distinct waves can be exploited for all-optical signal processing both in the plane wave limit and in the spatial solitary-wave case. For the specific case of Type II Second-Harmonic Generation in bulk KTP, we have predicted and demonstrated all-optical transistor action with small signal gain and angular steering and switching of spatial simultons. All the phenomena rely exclusively on inputs at the same fundamental frequency.

Three-wave interactions through a quadratic nonlinearity encompass several important phenomena, from new frequency generation to parametric amplification. In the context of all-optical processing, the use of two (out of three) input waves allows the exploitation of these coherent effects without the requirement for a precise control of the relative phases, *i.e.*, permitting to control the interaction outcome by only varying the relative number of photons in the two injected waves. With specific reference to the frequency degenerate case of Second-Harmonic Generation (SHG), the three-wave character is retained in the vectorial case, *i.e.*, when a Type II phase-matching scheme can be implemented. Two fundamental frequency (FF) waves, with electric fields either orthogonally polarized or corresponding to two orthogonal guided-wave eigenmodes, can interact through SHG and produce a throughput which depends on the photon imbalance at the input. When this is implemented in the plane wave limit, for instance, by using a collimated laser beam propagating through a relatively thin nonlinear crystal as KTP, additional effects such as birefringent walk-off, diffraction and dispersion (when pulses are employed) can be neglected, and a variation in input imbalance will result in a significant change in throughput, provided the SHG interaction is nearly phase-matched [1], [2]. Conversely, when the parametric gain overcomes both walk-off and diffraction in a longer crystal, solitary waves will form [3],

[4] and propagate along a direction depending on the prevailing polarization component at launch. A variation in imbalance will therefore result in angular steering of the spatially self-guided nonlinear solution in the walk-off plane.

The equations describing the three electric field amplitudes for Type II *eo*e SHG in a birefringent crystal (such as KTP) can be written in the form

$$\delta_z \begin{pmatrix} E_o^\omega \\ E_e^\omega \\ E_e^{2\omega} \end{pmatrix} - \delta_x \begin{pmatrix} 0 \\ \rho^\omega E_e^\omega \\ \rho^{2\omega} E_e^{2\omega} \end{pmatrix} + \frac{\Delta_l^2}{2i} \begin{pmatrix} E_o^\omega/k_o^\omega \\ E_e^\omega/k_e^\omega \\ E_e^{2\omega}/k_e^{2\omega} \end{pmatrix} = i\Gamma \begin{pmatrix} E_e^{2\omega}(E_e^\omega)^* e^{-i\Delta k z} \\ E_e^{2\omega}(E_o^\omega)^* e^{-i\Delta k z} \\ 2E_o^\omega E_e^\omega e^{i\Delta k z} \end{pmatrix} \quad (1)$$

with the walk-off angle ρ^ω and $\rho^{2\omega}$ defined in the *x-z* plane, $\Delta k = k_e(2\omega) - k_e(\omega) - k_o(\omega)$ the wavevector mismatch and Γ the nonlinear coefficient. In the KTP, $\Gamma = 6 \text{ cm}^{-1}$ for a 1 GW/cm^2 FF input, $\rho^\omega = 0.18^\circ$, $\rho^{2\omega} = 0.28^\circ$ for an operating wavelength of $1.064 \text{ }\mu\text{m}$. In the plane wave limit diffraction and walk-off (second and third terms on the LHS of (1)) can be ignored, although additional spatial and temporal integrations are required to take into account the laser beam distribution and the temporal envelope of the incident pulses. For the case of solitary waves, the system (1) can be solved using a split-step beam propagator accounting for both transverse dimensions.

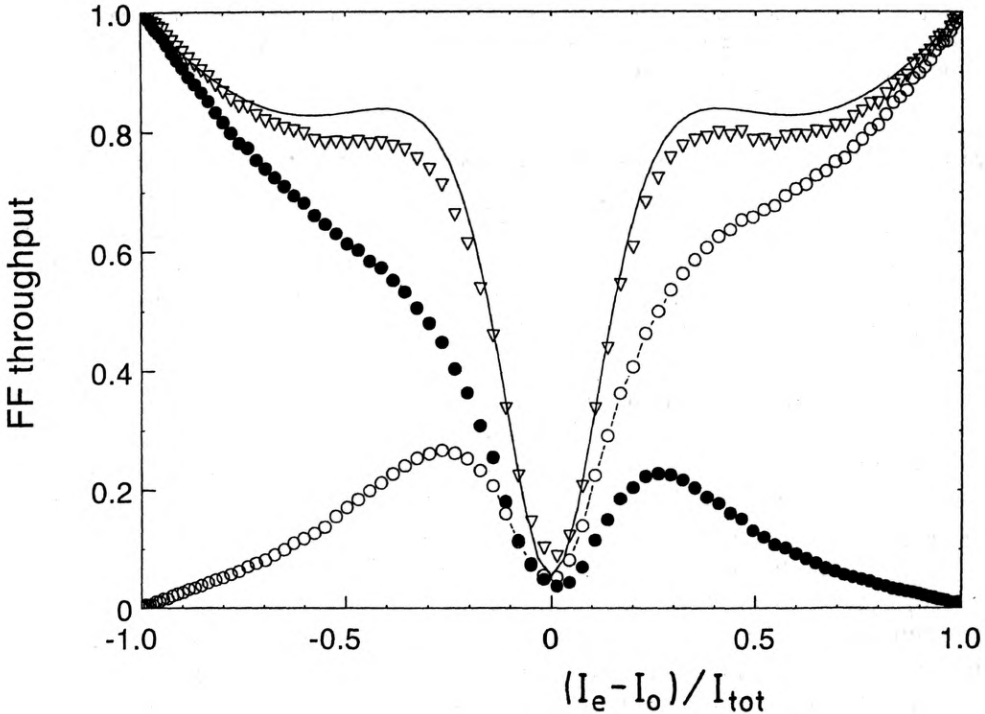


Fig. 1a

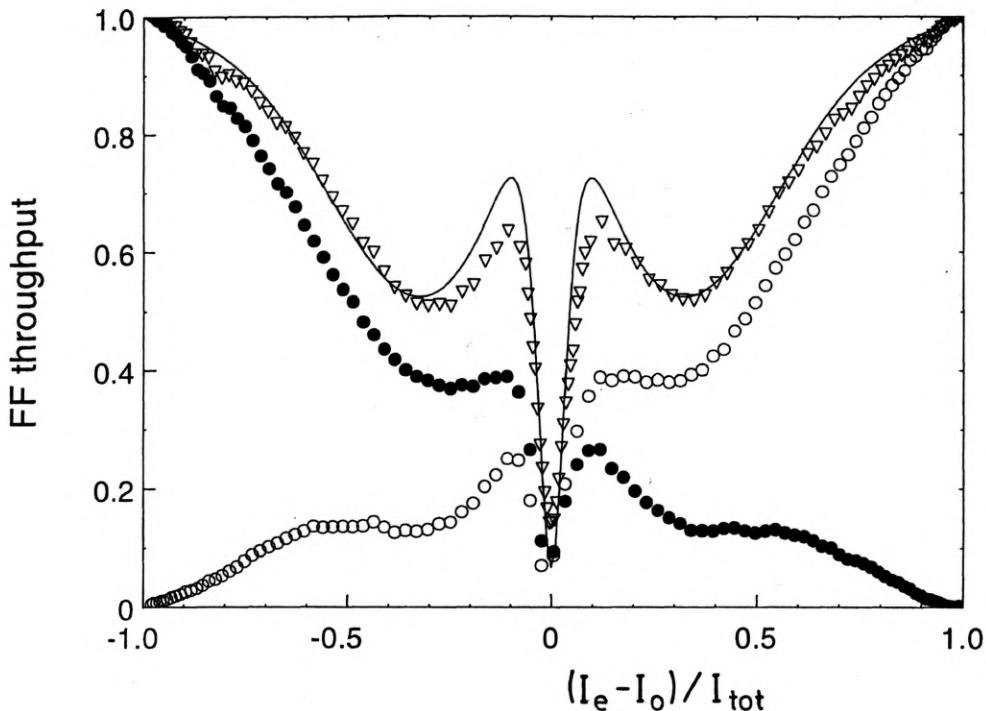


Fig. 1. All-optical transistor response through Type II SHG in KTP. The horizontal axes are in units of imbalance $(I_e - I_o)/I_{tot}$ between e and o inputs, and the vertical axes are normalized to the linear values. Hollow and filled circles represent the throughputs in the two orthogonal polarizations, whereas triangles and the solid line refer to measured and computer simulated total transmission, respectively. a - total FF input intensity $I_{tot} = 6 \text{ GW/cm}^2$, b - $I_{tot} = 12 \text{ GW/cm}^2$

A first set of experiments were conducted in the plane-wave limit in order to demonstrate transistor action as predicted numerically and analytically [1], [2]. Measurements were performed with a linearly polarized Nd:YAG Gaussian beam of wavelength $1.064 \mu\text{m}$ and waist $80 \mu\text{m}$. The Q-switch mode-locked source generated 25 ps pulses at 10 Hz rep-rate, and half-wave plate was put in front of a 2 mm-long KTP crystal in order to vary the FF imbalance between e and o input components by a simple rotation. Initially, the crystal and the electric field were aligned in order to maximize SHG, with an angle of 45° at the input facet. After setting an imaging system (5X) and a $100 \mu\text{m}$ pinhole at the output of the crystal in order to reduce the effects of spatial averaging, we measured the total throughput versus imbalance (i.e., waveplate rotation) for various total FF fluences. Figure 1 shows the experimental results and the theoretical calculations, having introduced the wavevector-mismatch as an adjustable parameter. The FF transmittance is normalized to its linear value, and no corrections were introduced for angular or temporal walk-off. The results exhibit an abrupt switching feature about zero imbalance, which becomes sharper and sharper as the input fluence is increased, with a transmission contrast as high as 7:1 for a 1° change in input angle (0.5° waveplate rotation). This corresponds to

a small signal amplification of 14 dB when varying the amplitude of one of the inputs as the other is kept constant [5]. The overall comparison between the model and the experimental results is quite satisfactory for a mismatch ΔkL between 0.05 and 0.1π .

This simple all-optical transistor scheme, however, operates at its best in the vicinity of zero imbalance, thereby requiring the signal to be a small coherent modulation of a large background input [2]. Therefore, in order to operate with an actually small signal with no coherent offset, a modulator stage has to transfer it onto a cw wave of amplitude comparable to that of the unmodulated input in the transistor above. A configuration of this sort is shown in Fig. 2, with a Type II "modulator" (1st crystal) stage which prepares the signal + offset input to the second "amplifier" stage (2nd crystal). Polarization sensitive optics are required to accommodate for the fields orientation with respect to the crystal axes. This geometry

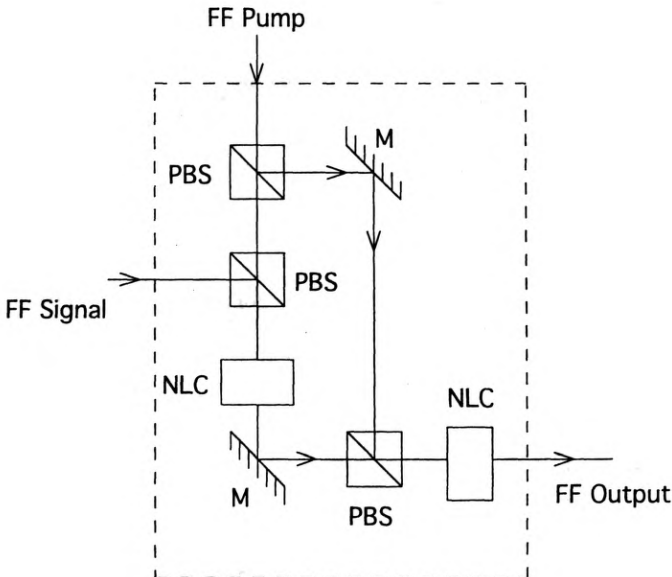


Fig. 2. Two-stage scheme for an all-optical transistor with phase unrelated signal and pump at the same frequency. NLC — nonlinear crystal for Type II SHG, PBS — polarizing beam splitter M — mirror

allows the incoherent (*i.e.*, phase insensitive) amplification of an arbitrarily small FF signal by means of a strong pump of the same frequency [6]. This version of the transistor is presently being demonstrated.

Let us now turn to the spatial solitary wave (SSW) case. Solitary waves in the presence of quadratic nonlinearities have been the subject of extensive investigations, especially after their initial experimental demonstration in KTP and lithium niobate [3], [4]. When the beams interacting through SHG experience a parametric gain which prevails on linear diffraction and walk-off, all the wave-components (at FF and SH) coalesce into a self-guided bifrequency eigenmode (or simulton). According

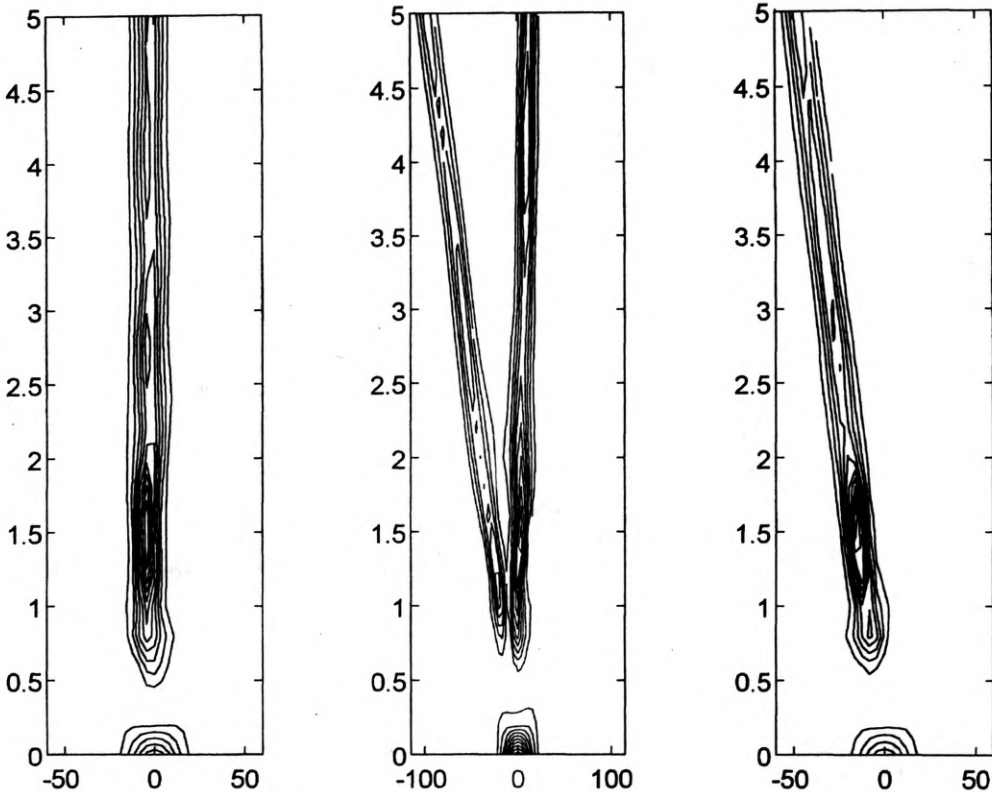


Fig. 3. BPM numerical simulation of the propagation of spatial solitary waves due to Type II SHG in KTP. The contour maps represent FF intensity versus propagation distance (in diffraction lengths) and transverse coordinate x in μm , for $I_e = 20 \text{ GW/cm}^2$ and $I_e = 18.5 \text{ GW/cm}^2$ (left); $I_e = 19.5 \text{ GW/cm}^2$ (center), and $I_e = 20.5 \text{ GW/cm}^2$ (right)

to this intuitive picture, when both ordinary and extraordinary rays are permitted, a field-bias in one or the other polarizations should allow to change the direction of propagation of the overall SSW, as predicted by a BPM solution of system (1). A variation of the input FF imbalance, then will provide the angular steering of the SSW and its lateral displacement at the end of the crystal. Figure 3 shows typical results of the simulations, including an intermediate double-hump state permitted only for input more than a factor two larger than the single SSW threshold. The slight asymmetry with respect to zero imbalance is due to the presence of natural walk-off in the e components. Figure 4 displays the experimental results obtained with a set-up similar to the one described above, but with a beam waist of $12 \mu\text{m}$ into a 1 cm crystal and an IR camera at the output. The figure shows a cross-section of the output plane along the walk-off direction x . Clearly, the expected features are well reproduced, with a measured lateral displacement of as much as $80 \mu\text{m}$ for total intensities $I_{\text{tot}} = 80 \text{ GW/cm}^2$. When an aperture was placed on either side of the crystal exit facet, a switching contrast exceeding 10 was obtained for input modulations of less than 20% [7].

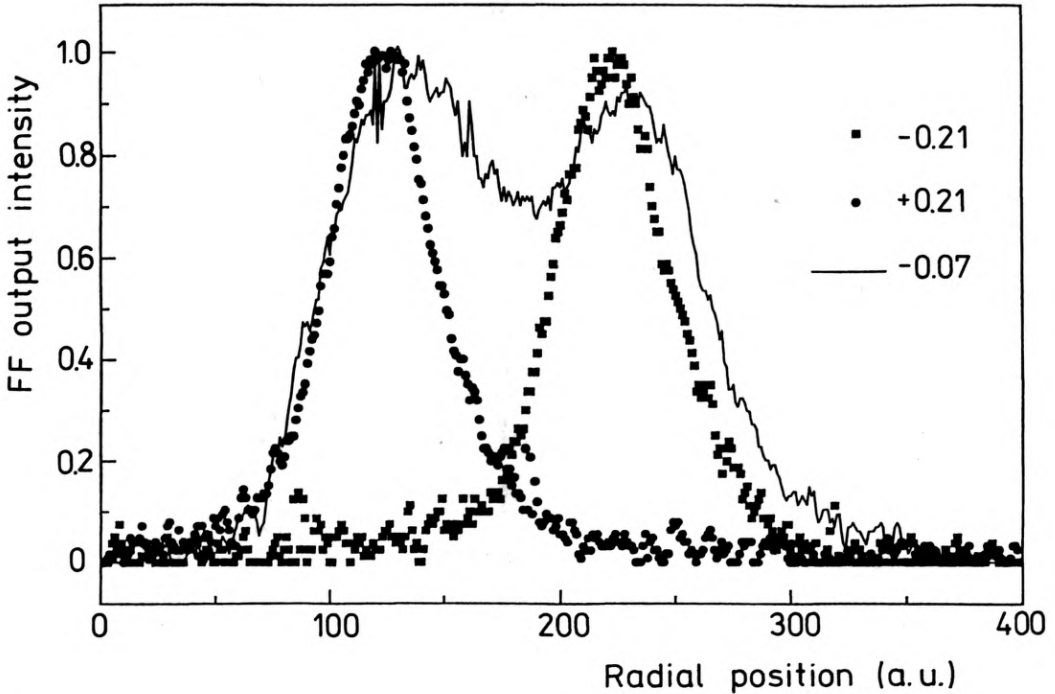


Fig. 4. Measured intensity profiles of SSW at the output of the KTP crystal along x . The legend in the insert indicates the intensity imbalance ($I_e - I_o / I_{tot}$ for $I_{tot} = 80 \text{ GW/cm}^2$)

In summary, the suitability of vectorial quadratic interactions for frequency-degenerate and phase-insensitive all-optical signal processing has been experimentally verified through Type II SHG in KTP bulk crystal, both in the quasi-plane wave and in the solitary wave limits. An intensity imbalance in the orthogonal components of the beam entering the crystal can severely modify the character of the process regardless of the relative input phase. This results into throughput modulation and small-signal gain in the plane-wave approximation, *i.e.*, into all-optical transistor operation. When larger intensities and longer propagation lengths are employed, the formation of spatial solitary waves lends itself to an imbalance control of their direction of propagation, which results in intensity-driven angular steering and switching. Novel materials with higher nonlinearities and reduced walk-off and the adoption of guided wave geometries will certainly allow to exploit the above effects at much lower excitation levels, opening the way to affordable all-optical signal processing schemes and reconfigurable 2D interconnects.

Acknowledgements — We are indebted to B. L. Lawrence, G. Leo and Z. Wang for their important contributions to this work. G. A. acknowledges support from the Italian Research Council (95.04118.CT11, 95.00031.CT07) and MURST (40% Photonic Technologies). G. A. and E. W. V. S. are also grateful for a NATO grant (CRG 931142).

References

- [1] ASSANTO G., *Opt. Lett.* **20** (1995), 1595.
- [2] KOPYAKOV A., PESHCEL U., MUSCHALL R., ASSANTO G., TORCHIGIN V. P., LEDERER F., *Opt. Lett.* **20** (1995), 1686.
- [3] TORRUELLAS W. E., WANG Z., HAGAN D. J., VAN STRYLAND E. W., STEGEMAN G. I., TORNER L., MENYUK C. R., *Phys. Rev. Lett.* **74** (1995), 5036.
- [4] SCHIEK R., BAEK Y., STEGEMAN G. I., *Phys. Rev. E* **53** (1996), 1138.
- [5] ASSANTO G., WANG Z., HAGAN D. J., VAN STRYLAND E. W., *Appl. Phys. Lett.* **67** (1995), 2120.
- [6] WANG Z., HAGAN D. J., VAN STRYLAND E. W., ASSANTO G., *Electron. Lett.* **32** (1996), 1135.
- [7] TORRUELLAS W. E., ASSANTO G., LAWRENCE B. L., FUERST R. A., STEGEMAN G. I., *Appl. Phys. Lett.* **68** (1996), 1449.

Received November 27, 1996